

System Level Considerations for Integration of Resonant Capacitors in High Power Wireless Charging

Michael A. Brubaker, Hugh C. Kirbie, Terry A. Hosking, and Ted Von Kampen
SBE Inc., 81 Parker Road, Barre, Vermont, 05641; (802) 661-3501
email: powerring@sbelectronics.com
File transfer site: www.sbelectronics.com

ABSTRACT

Mass adoption of electric vehicle technology is highly dependent upon ease of recharging at the consumer level. Various strategies including battery swapping, improved battery efficiency, and wireless charging have emerged to address this issue. In the context of wireless charging, implementation options range from local hotspots in the user's garage or public parking areas to energized roads. While a great deal of attention has been focused on the coupling coils and drive circuitry for wireless charging, the resonating capacitors are equally important components and must be carefully considered. Typical resonant frequencies range from 10 kHz to over 150 kHz which can be supported by both film and ceramic capacitor technology. However, there are significant compromises between cost and performance that remain to be clearly defined. Furthermore, capacitor performance can be significantly impacted by the hostile operating environment, which will include heating from stray magnetic fields and high-temperature coil components. An investigation of optimized hybrid film/coil capacitors has been undertaken to define the frequency and voltage operating regime where stability, cost, and graceful aging can balance dissipation losses. Test results for polypropylene film capacitors in a coupled coil resonant circuit are presented along with discussion of system level implementation.

INTRODUCTION

Wireless charging of moving or stationary electric vehicles is considered by many to be an enabling technology that will provide convenience and thus expedite mass market acceptance. A variety of wireless charging techniques have been developed to date¹⁻³, with the dominant approach at the vehicle scale being magnetically coupled coils. While a number of different coil and drive architectures are available, the common feature in this approach is the requirement for resonance to achieve efficient energy transfer. The capacitors needed for resonant coupling are thus an essential component that must be understood for this application. In particular, very low loss capacitors are important to avoid spoiling the Q of the circuit and reducing efficiency.

While significant effort has been devoted to optimizing coil designs for wireless charging, the resonating capacitors have traditionally received much less attention. The purpose of this paper is to provide some insight into parameters that must be kept in mind for capacitor selection including losses, stability, voltage, frequency, self-healing, hot spot temperature rise, reliability, and thermal management. As wireless charging technology moves to commercialization, capacitor cost becomes an important factor which must be carefully traded against performance.

Furthermore, resonating capacitors must be assessed at the system level in order to achieve the most optimal solution.

An overview of the capacitor requirements for wireless charging indicates that ceramic and film constructions are the best commercially available candidates. New materials have not been considered in this discussion given the desire to deploy a wireless infrastructure over the near term of three to five years. A comparison of ceramic and dry film technologies is provided from which the latter emerges as the logical choice in terms of cost and performance. An analysis of different film capacitor configurations supports the next level of down selection as film/foil, which offers better thermal performance than single or double metalized. Test results are presented for an optimal film/foil "building block" in different series-parallel combinations over a relevant range of frequency and voltage with different thermal boundary conditions. The analysis and test results provide a basis for discussion of capacitor integration at the system level, which addresses stray field effects, optimal interconnections, and thermal management. An optimized film/foil capacitor with the right infrastructure is shown to provide the best compromise between cost and performance for high power wireless charging.

CAPACITOR REQUIREMENTS

High power wireless charging is a demanding application from the capacitor perspective. Consider the following list of desired parameters:

1. **Tight tolerance** – The ability to match the capacitor to the coil at the desired resonant frequency is needed to minimize adjustment and tuning. This is also important for voltage balancing when combining capacitors in series for higher voltage.
2. **Ability to fabricate specific values** – Commercial capacitors are typically supplied in very specific value increments, which may limit the selection of a resonant frequency. Also, the ability to make larger values in a single monolithic part is desirable to simplify assembly.
3. **Low losses** – Capacitor losses will generate heat in the charging system and can also contribute to a reduction in the quality factor of the resonant circuit.
4. **High AC rms capacitor operating voltage** – The desire to minimize the coil current typically requires a higher voltage to be applied across the capacitor. Higher voltages will necessitate using multi-section capacitor designs, which requires good balancing of the capacitance values to avoid overstress problems. Mismatch can cause corona initiation in the over-stressed section, which will significantly reduce life.
5. **Low temperature coefficient** – An outdoor system can experience ambient operating temperatures in the range of -40°C to $+85^{\circ}\text{C}$. The capacitance value should ideally be stable over this range plus higher internal system temperatures to avoid tuning problems.
6. **Low voltage coefficient** – Many ceramic dielectrics exhibit a change in dielectric constant with applied voltage, which will affect the capacitance and resonant frequency.
7. **High operating temperature** – Wireless charging systems have components located on the vehicle and on a base station. The minimum possible cooling infrastructure is desired while keeping the capacitor hotspot within safe operating limits. Note that the hotspot temperature typically exceeds the ambient by some amount.
8. **Good thermal properties** – A low thermal resistance in the capacitor section is ideal to minimize the hotspot temperature rise. Applications requiring an intermittent duty cycle (e.g. energized road) can also benefit from a large thermal time constant, so a high specific heat may be useful.
9. **Wide frequency range** – Commercial systems are now operating from 10 kHz to 150 kHz.
10. **Environmentally friendly** – The use of insulating oil, lead, or ozone depleting materials should be avoided.
11. **Commercially available materials and technology** – The resonating capacitors should be proven technology that is ready for deployment today.
12. **High reliability** – Reliability is critical for consumer acceptance of wireless charging. Graceful aging of capacitors (self-healing and gradual capacitance loss) over long life rather than periodic component replacement is essential. Given the high AC voltage requirements, the capacitors must be corona free at nominal voltage to avoid rapid aging problems.

The capacitor selection is further complicated by the need to achieve the best possible performance at the lowest possible cost.

CAPACITOR TECHNOLOGY SELECTION

Some very good overviews of capacitor technologies are available in the open literature^{4,5} which address ceramic, film, paper, and electrolytic parts. At first glance, electrolytic capacitors can be eliminated for this application given the requirement for AC voltage. Given environmental concerns, oil impregnated capacitors can also be taken off the list, thus eliminating paper and wet film options. Note further that wet film capacitors are typically supplied in metal cans, which help with heat transfer, but are not desirable in a stray magnetic field application. This leaves only ceramic and dry film as the remaining contenders for wireless charging applications. Both of these technologies are mature and commercially available from multiple vendors. Consider X7R (BK) and NPO (COG) class ceramic capacitors as compared with polyester (PET) and polypropylene (PP) film in Table 1.

Table 1. Comparison of common ceramic and film capacitor parameters based on industry datasheets

Parameter	X7R (BK)	NPO (COG)	PET	PP
Tolerance ^a	+/- 10%	+/- 1%	+/- 1%	+/- 1%
Custom values ^b	Large run	Large run	Wind to value	Wind to value
Losses ^c	7% - 0.2% DF -55°C to +125°C	0.07% - 0.1% DF -55°C to +125°C	0.2% - 1.4% DF -55°C to +125°C	0.02% - 0.04% DF -55°C to +105°C
AC Voltage ^d	>5 kV	>5 kV	>5 kV	>5 kV
Temperature Coefficient ^e	+/- 15 % -55°C to +125°C	+/- 30 ppm/°C -55°C to +125°C	-6% to +20% -55°C to + 125°C	- 200 ppm/°C -55°C to +105°C
Voltage Coefficient ^f	<-10% DC > 10% AC	< 0.02%	Negligible	Negligible
Max Operating Temperature ^g	125°C	125°C	125°C	105°C
Thermal Properties ^h	k = 4 W/m/°C	k = 4 W/m/°C	k = 0.2 to 100 W/m/°C	k = 0.2 to 100 W/m/°C
Typical Operating Frequency Range ⁱ	DC – 10 MHz +4% to -15% °C 10% DF	DC – 10 MHz +0.05% °C .08% to +0.17 DF	DC – 150 kHz +0.8% to -6% °C 0.2% to 3% DF	DC – 150 kHz -2% °C 0.02% to 0.03% DF
Environmental	Good	Good	Good	Good
Commercial	Yes	Yes	Yes	Yes
Reliability ^j	Aging Hard fault	No Aging Hard fault	Graceful Aging Self-healing	Graceful Aging Self-healing

^aCeramic data based on survey of typical industry datasheets. While +/-1% NPO is available, the most common tolerance is +/- 5%. Film data based on SBE experience with winding tight tolerance film capacitors.

^bCeramic data based on survey of typical industry offerings. On the film side, SBE has significant experience winding to value for tight tolerance parts.

^cFilm and ceramic data based on surveys of typical industry datasheets.

^dBoth film and ceramic parts (sections) can be combined in series to provide a higher voltage rating provided that the capacitance values are well balanced. If the capacitance tolerance is poor, the lowest capacitance section will take on a higher proportionate share of the applied voltage, which reduces the service life.

^eCeramic data based on the EIA definitions for X7R and NPO class. PET and PP film values from SBE internal data with additional confirmation from the open literature⁵.

^fCeramic data based on survey of typical industry datasheets with values shown for approximately 100 V (AC or DC). Large coefficients are normally reported for higher voltages. Film capacitors have a negligible voltage coefficient when operated at stress levels

well below breakdown. Polypropylene is particular has a very minimal effect since the polarization in this case is defined by electron motion.

^gCeramic data based on survey of typical industry datasheets and EIA requirements. Film capacitor data from SBE experience. Operating temperature is important to minimize the cost of the cooling infrastructure. Self-heating will raise the hotspot temperature above the operating temperature.

^hFilm capacitor thermal conductivity in the axial direction depends on ratio of film to electrode material. Ceramic capacitor data based on typical industry datasheets (thermal conductivity is isotropic).

ⁱFor film capacitors the high frequency operation is limited by increased dissipation and thermal management rather than changes in dielectric constant.

^jMetalized film capacitors offer the unique feature of self-healing. When a defect occurs, the resulting fault current vaporizes the local electrode region, thus effectively isolating the defect location. The removal self-healing regions is insignificant for solid metalized film, but causes more capacitance loss in the case of segmented metallization.

Based on the comparisons in Table 1, the best respective choices for film and ceramic are polypropylene and NPO, both of which are available to 1% tolerance. NPO offers somewhat better temperature and frequency stability along with a higher maximum operating temperature. However, PP has significantly lower losses in the 150 kHz range and can be easily wound to any desired capacitance value. Moving into higher frequencies above 200 kHz, the dissipation factor (DF) for PP film exceeds that of NPO. Beyond this crossover point in frequency, a good case can be made for the use of ceramic with regard to heat loading. However, in the range of 10 kHz to 150 kHz presently under consideration for wireless charging, PP film provides a lower DF with the added advantage of self-healing.

The critical decision point ultimately comes down to reliability, where PP film is superior given the ability to age gracefully by virtue of self-healing. NPO does not exhibit significant aging effects, but when a defect occurs, this type of capacitor will fault and fail without the ability to recover. In some cases, the ceramic reliability issue is addressed by de-rating, which comes with a cost and volume penalty. The same discussion applies for a variety of other high power resonant converter applications where film capacitors are typically utilized⁷ for high reliability, good stability, and low equivalent series resistance (ESR)⁸. Finally, film capacitors offer a cost savings of 50% or better for applications exceeding approximately 0.5 kW.

OPTIMIZED FILM FOIL HYBRID DESIGN

Assuming that polypropylene film represents the best overall dielectric selection in the frequency range of interest, the optimal film capacitor design for high power wireless charging remains to be defined. The determining factors at this point become the operating voltage and thermal resistance. The maximum practical capacitor section voltage for a dry film capacitor is 250 VAC rms for adequate film thickness. Recognizing that some wireless systems require voltages of 2000 VAC or higher, a multi-section design is required. Note that this implies sections having very well matched capacitor values to avoid overstress problems. The specific arrangement of the sections is very important for heat transfer to external connection points. In this regard, the use of a two-section “building block” winding rated for 500 VAC is the optimal approach, which is explained in the following paragraphs.

Two layers of a two-section single-metalized film capacitor design are illustrated in Figure 1a, which shows the film, electrodes, and end connections. Note that an exaggerated air gap has been shown between the film layers to make the diagram easier to interpret and the exact nature of the electrode and end connections is has not been defined. The effective or active width where the electrodes on each side of the film overlap defines the capacitance per layer in conjunction with the film thickness and mean radius. The end margin and center separation are required to provide suitable isolation between electrodes of opposing potential. This is an “even order” design such that both margins are applied onto the same film layer and no offset between the films is required. An extension of the end metallization film layer beyond the common layer on each edge provides for an external connection via arc spraying.

The thermal performance of the design is dictated by the ratio of the electrode and film thicknesses. A thicker electrode offers the advantage of reduced electrode (Ohmic) losses combined with a higher axial thermal conductivity. The latter point drives the choice of a two-section design such that each section has a short thermal path to an end connection that provides an access point for external cooling. With this in mind, a more detailed discussion of the capacitor losses can be undertaken. Consider the common (bottom) electrode in Figure 1a for the left hand section. Starting at the margin side and working toward the separation, the displacement current from the top electrode increases linearly. This leads to a parabolic power density distribution given as

$$\text{Power Density} = \frac{4\epsilon^2 z^2}{d^2 t} \left(\frac{I}{C}\right)^2 R_s$$

where

ϵ = permittivity of the film (F/m)

z = axial distance from left hand margin (m)

d = film thickness (m)

t = electrode thickness (m)

I = total capacitor current (A)

C = section capacitance (F)

R_s = sheet resistance (Ω /square).

Exactly the opposite distribution will exist in the top electrode, but the power density for the separation and margin electrodes will be constant in z and defined by the section current in the layer flowing through the appropriate resistance. Integrating the layer results across the complete capacitor volume and accounting for both sections, both margins and the separation gives the total electrode losses as

$$P = \frac{4 \text{ EWF}}{3 \text{ ELF}} I^2 R_s + 2 \frac{\text{MARGIN}}{\text{ELF}} I^2 R_s + \frac{\text{SEPARATION}}{\text{ELF}} I^2 R_s$$

where the EWF is the effective width of the film in each section and the ELF is the total length of film in the winding. The other loss contribution comes from dielectric dissipation in the film, which is independent of the electrode construction and depends purely on the stressed area. The dissipation is uniformly distributed in the active region of each section and the corresponding total power is

$$P = \frac{DF}{\omega C} I^2$$

where DF is the dissipation factor and ω is the angular frequency.

Having defined the losses, the next aspect is the thermal resistance of the winding, which determines the temperature rise relative to the end connection as a function of the total losses. Intuitively, one would expect the thermal resistance to correlate with the electrode sheet resistance. While this is indeed the case, the ratio of film to electrode volume complicates the relationship. Consider one layer of film and the associated electrode shown in Figure 1a. The axial thermal resistance per unit length of film in the wind

direction and per unit width in the axial direction for each material in the active region is defined by the thermal conductivity k and the thickness t as

$$R_T = \frac{1}{k t}$$

If we denote the electrode with the subscript “e” and the film with the subscript “f”, the parallel combination of the thermal resistances for each layer provides the effective thermal conductivity as

$$k_{\text{effective}} = \frac{k_f \left(1 + \frac{k_e t_e}{k_f t_f}\right)}{\left(1 + \frac{t_e}{t_f}\right)}$$

Note that the thermal resistance is further complicated at the ends of the sections by the alternating margin and separation layers. However, the effective thermal conductivity of the active area is very useful to define a figure of merit for axial heat transfer.

At this point, the details of the electrode configuration must be further defined. There are essentially three possible constructions to be compared:

1. **Metalized** – The electrodes are directly vapor deposited on the film layers (see Figure 1a). This approach offers the best capacitance density, but has the lowest electrode to film ratio. The end connections are arc-sprayed to connect with the film electrode extensions.
2. **Double Metalized** – In this case, the electrodes are realized using film layers that have been metalized on both sides to provide more electrode thickness. This design uses arc-sprayed end connections (see Figure 1b). Note that the carrier film for the electrodes is not part of the dielectric system, so a higher temperature material like PET can be used.
3. **Foil/Metalized** – Foil electrodes are used for the layer where the end connections are brought out (see Figure 1c). Foil ends are arc-sprayed to eliminate wind direction current flow and provide the best thermal and electrode connection. The “common” electrode is made using a double metalized film rather than foil. This allows the part to

self-heal on the common layer for graceful aging with the maximum ratio of electrode to film. This provides lower losses, improved heat transfer, and less local heating of the dielectric when self-healing occurs.

In order to compare the three electrode options, consider a 1 μ F capacitor operating at 10 kHz and a 10 nF capacitor operating at 100 kHz. For each case, assume the following parameters:

1. EWF = 10 mm
2. Applied voltage = 500 VAC across the winding (250 VAC per capacitor section)
3. Film thickness = 10 μ m
4. Common electrode thickness = 5 μ m
5. Sheet resistance for metallization on film = 2 Ω /sq
6. Foil thickness = 5 μ m (where applicable)

The losses, effective thermal conductivity, and effective thermal resistance are compared for each capacitor construction option in Table 2. The effective thermal conductivity of the film/foil construction is two orders of magnitude higher than the double metalized. Note that the relationship between effective thermal conductivity and thermal resistance depends on the total cross sectional area of the winding. Note further that the dissipation losses depend on the stressed area of the dielectric (capacitance) and are thus the same for all three cases. However, the film/foil construction provides much lower electrode losses, which become significant due to increasing current as the frequency is increased. To be precise, the film/foil electrode losses are a factor of two less than the double metalized and a factor of four less than the single metalized. Similarly, while double metalized provides half the thermal resistance of single metalized, the foil construction is more than 10 times better than double metalized. From a cost perspective, single metalized is the least expensive construction, and the relative price increment to double-metalized is typically 10-25%. However, film/foil is cost equivalent to double-metalized, thus offering superior performance at the same price.

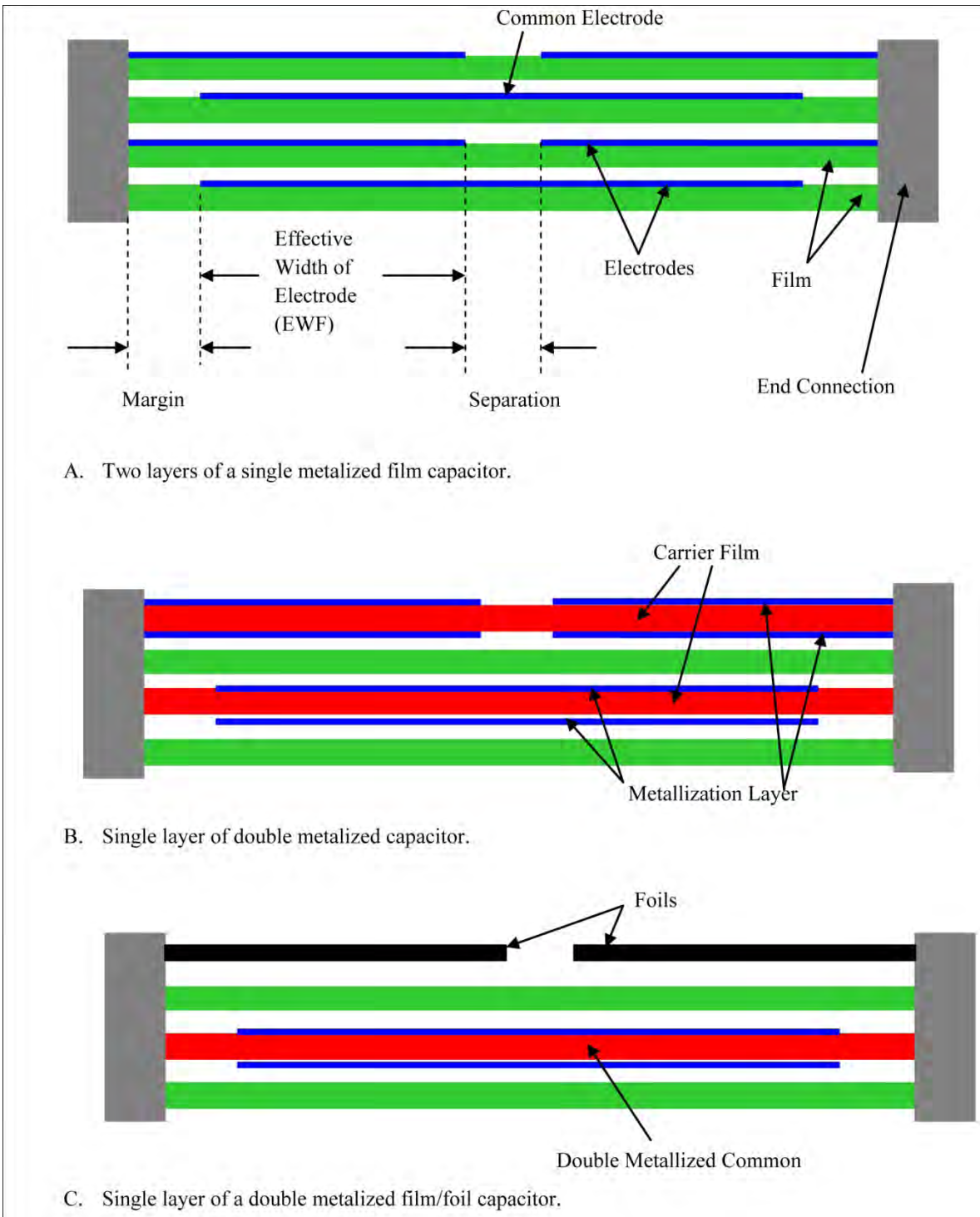


Figure 1. Illustration of two-section film capacitor constructions

Table 2. Comparison of losses and thermal performance for three common film capacitor constructions versus value and frequency

Parameter	Single Metalized 10 kHz	Single Metalized 100 kHz	Double Metalized 10 kHz	Double Metalized 100 kHz	Film/Foil 10 kHz	Film/Foil 100 kHz
Capacitance (μF)	1	0.01	1	0.01	1	0.01
Electrode Losses (W)	0.70	0.70	0.35	0.35	0.17	0.17
Dissipation Losses (W)	3.14	0.31	3.14	0.31	3.14	0.31
Total Losses (W)	3.84	1.02	3.49	0.67	3.31	0.48
k_{eff} ($\text{W}/\text{m}^2/\text{C}$)	0.53	0.53	0.65	0.65	40.4	40.4
R_T ($^\circ\text{C}/\text{W}$)	16.3	1630	8.97	897	0.14	14.4

FILM/FOIL CAPACITOR TESTING

Having demonstrated that the film/foil capacitor with a double metalized common electrode is the best selection for wireless charging, an experiment was constructed to evaluate thermal performance. A two-section film/foil part was designed as the “building block” for the test program and a production run of 100 pieces was undertaken. Selected capacitors were then instrumented with thermocouples to monitor the internal hotspot temperatures and the parts were assembled into arrays. The extended foils on the capacitor windings were bonded to the tinned copper end plates defining each stage using silver epoxy. A photograph of the three-stage array used for testing at 1500 VAC is presented in Figure 2. Note that the arrays were installed in a climate chamber as illustrated for the three-stage part in Figure 3. Each array was tested while connected across a 93 μH litz wire coil wirelessly coupled to a drive coil supplied by an amplifier with a function generator input as shown in Figure 4. A custom-built current transformer was used to monitor the current in the circuit. The test parameters for each capacitor array configuration are presented in Table 3. Note that the total losses for each case were estimated using the formulas developed in the previous section.

Table 3 Capacitor array values and losses with respect to operating voltage and resonant frequency.

Voltage (VAC)	500	1000	1500	2000
Array Capacitance (μF)	1.0	0.125	0.033	0.0125
Series Stages	1	2	3	4
Parallel Windings per Stage	20	5	2	1
Resonant Frequency (kHz)	16.5	47.0	90.5	147.6
Per Winding Electrode Losses (W)	0.017	0.140	0.520	1.400
Per Winding Dissipation Losses (W)	0.259	0.739	1.420	2.320
Array Total Electrode Losses (W)	0.340	1.400	3.120	5.600
Array Total Dielectric Losses (W)	5.180	7.390	8.520	9.280

Tests were conducted for each array with two thermal boundary conditions, namely a static chamber at 25°C, an active chamber at 25°C. For the static case, the capacitors were allowed to reach approximate equilibrium relative to the chamber temperature without forced convection. In the active, case the capacitors were energized long enough for the system to reach equilibrium with forced convection cooling to the chamber temperature. Note that a separate thermocouple was used to monitor the chamber temperature to give a reference value for the capacitor hotspot rise. Note further that the thermocouples were read using battery powered hand-held units that were insulated to provide sufficient galvanic isolation from the electrical ground.

The maximum capacitor hotspot temperature results are summarized in Figure 5. As expected, the static chamber condition for each array provided the highest internal temperature rise. The addition of forced

convection in the chamber showed a significant reduction of the capacitor hotspot temperature for each case. While there was free or forced convection acting on the outer surfaces of the capacitor windings, this effect is second order due to the very poor thermal conductivity in the radial direction. The radial flow is limited to the bulk thermal conductivity of polypropylene that is further hampered by the air gap between layers, which is a function of film surface roughness and winding tension. Furthermore, the outermost foil layers are tightly coupled to the capacitor end temperature, which further limits the radial gradient. In contrast the axial thermal conductivity is significantly augmented by the foils and double metalized common electrode. As such, heat transfer via convection from the end plates defining the capacitor sections dictates the capacitor hotspot temperature.

Each winding in the array experienced the same applied AC voltage (500 VAC for all cases), which defined the electrode (Ohmic) and dielectric (dissipation) losses. The electrode losses increase as the square of the current, which varies linearly with the resonant frequency. The dissipation losses are directly proportional to the frequency. However, it is important to remember that the total losses are determined by the number of sections in the array. Clearly, having more parallel sections for higher capacitance reduces the electrode losses by virtue of parallel current paths. Conversely, more stages in series with fewer parallel windings for a larger array voltage at high frequency leads to increased electrode losses. It is interesting to note that the peak capacitor hotspot temperature occurs for the three-stage, rather than four-stage case. This is attributed to the ratio of the stage end plate area to the number of capacitor sections. The same plates were used for these two cases, which provided a larger convection surface for the four stage configuration. A similar argument can be applied for the low single stage array hotspot, which utilized larger plates with a better convection area. The single stage array also had strong conduction coupling through the interconnections to extract additional heat.

Another very interesting aspect of the capacitor thermal design can be determined by thermal imaging in the steady state. The three-stage array was tested again after being painted matte black to provide a defined emissivity on the surfaces and avoid false readings. The corresponding thermal image is shown in Figure 6 subject to a static chamber and room temperature ambient. The angle of view captures the capacitor interface on the underside of the plate connecting the second and third stage capacitors. This illustrates that the highest temperature in the array occurs at the interconnection between the plate and capacitor

sections. This results from the capacitor winding heat load coupling to the end plate via the internal foils. In effect, a temperature divider is created between the capacitor hotspot and ambient with the largest thermal resistance representing the convection coupling to ambient.

The arrays tested here serve to demonstrate what is possible over a realistic frequency and voltage range using film/foil capacitor technology. Clearly the capacitor construction and cooling must be optimized to suit specific applications with regard to configuration, thermal management, and interconnections. Ideally, each stage of the required array should be constructed using a single monolithic film Power Ring™ winding to provide the lowest cost. However, these test results show that a film/foil capacitor construction can be maintained well below the limiting hotspot temperature of 105°C with free or forced convection coupling to ambient. Electrically isolated end plates provide a very effective means of extracting heat from each capacitor section.

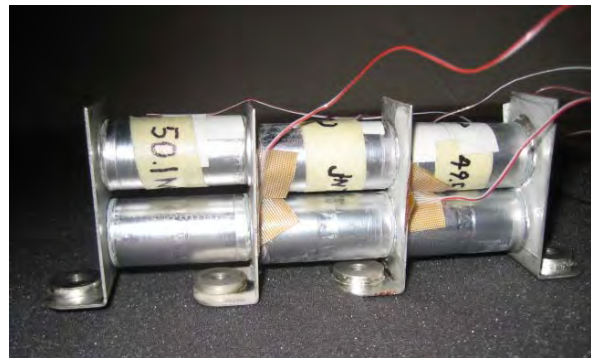


Figure 2. Three stage capacitor array rated for 1500 VAC showing thermocouples used to measure hotspot and end plate temperatures



Figure 3. Three stage capacitor array installed in climate chamber prior to testing

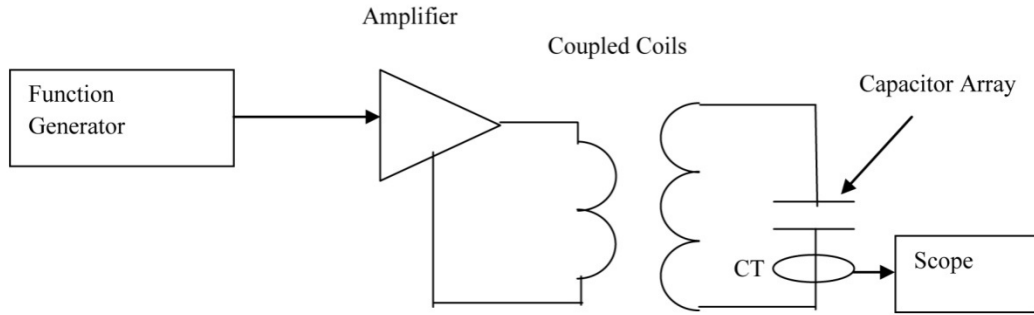


Figure 4. Schematic representation of the resonant test circuit

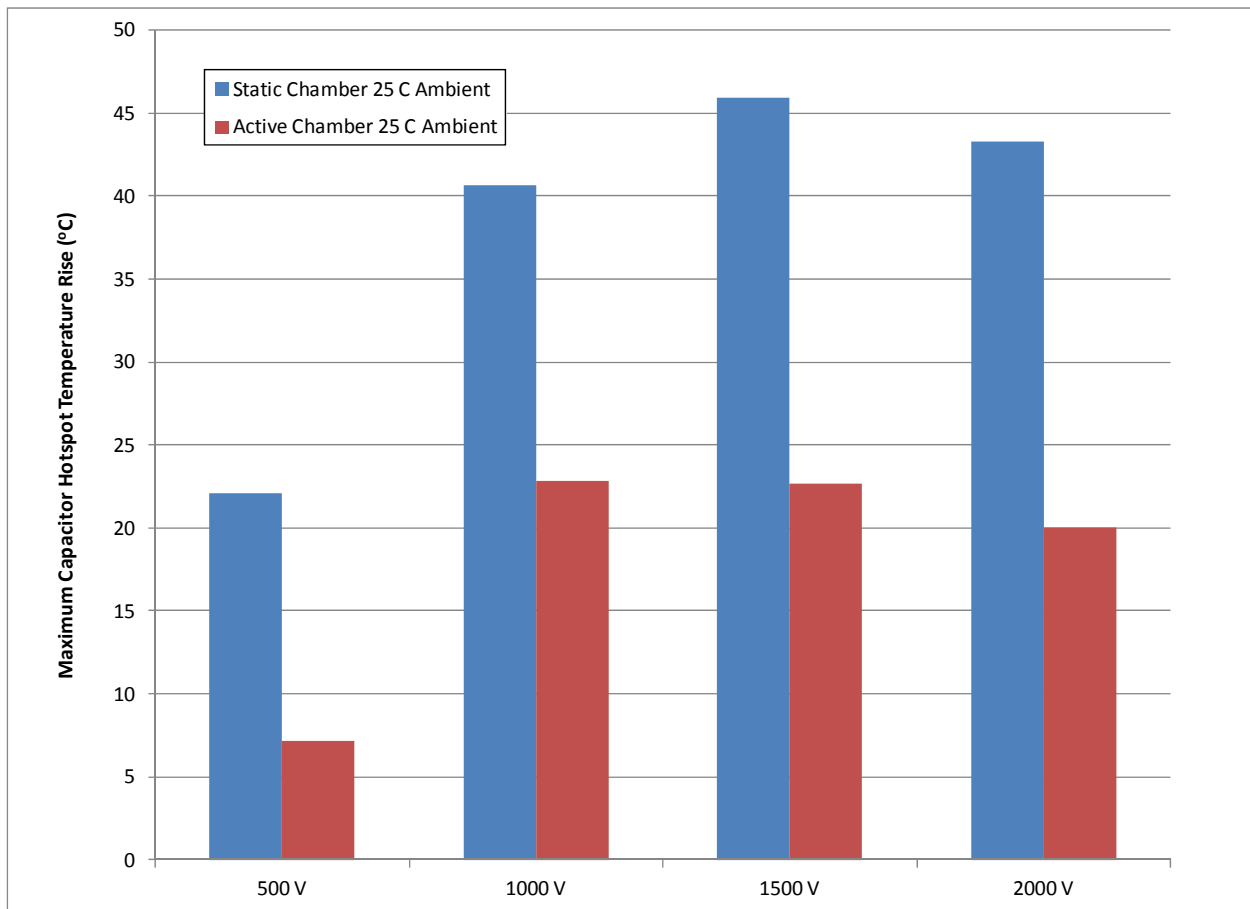


Figure 5. Capacitor hotspot temperature rise results subject to varying ambient conditions

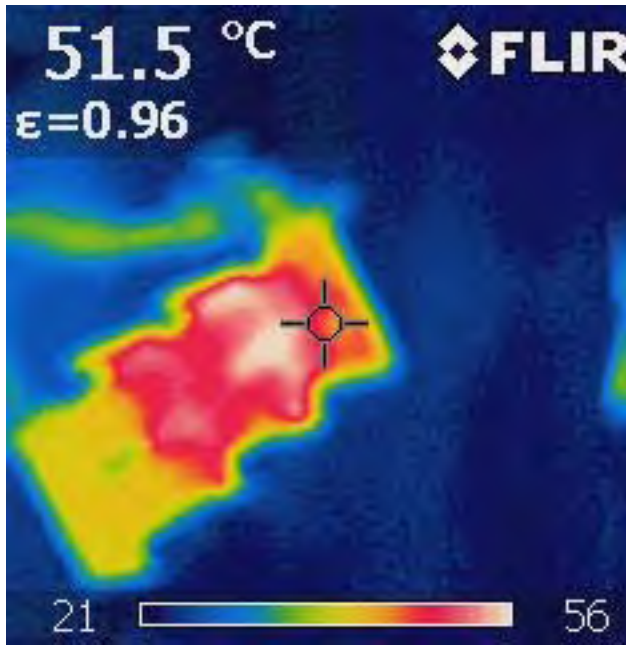


Figure 6. Thermal map of the three-stage array at equilibrium for room temperature ambient with static chamber

SYSTEM LEVEL INTEGRATION CONSIDERATIONS

The advantage of an optimal film/foil hybrid design has been demonstrated at both the conceptual and prototype test level. However, it is very important to realize the capacitor performance will be severely compromised if this part is not properly integrated into the wireless charging system. Even with the best possible capacitor design, problems can result from magnetic field interactions, improperly designed interconnections, and poor thermal management. These issues are discussed in more detail in the following subsections.

Magnetic field interaction

Faraday's law is well understood in the context of coupled coils for wireless charging. However, accepting that the divergence of the magnetic flux density must be zero, magnetic fields will be present outside of the coils. The normal component of magnetic flux density impacting any conducting surface will induce eddy currents and impart an added heat load. This is particularly important with regard to resonating capacitors, which are constructed using thin layers of foil and metalized film sandwiched between layers of insulation. Stray field effects can readily cause sufficient induction heating to melt the capacitor insulation. The damage location will correlate with the orientation of the winding that experienced the largest normal magnetic field component. Induction heating

can also occur in the plane of the end connections, which is orthogonal to the winding layers. It is important to understand that induction heating can pose problems for ANY type of capacitor (not just film) – even with a highly optimized design. The solution is to address the capacitor at the system design level with regard to orientation, interconnections, and thermal management. SBE ripple current testing of DC link capacitors has shown that induction heating effects can be almost completely eliminated with the correct interconnection geometry even with 20 kHz rms currents of 500 A.

Interconnections

This paper has demonstrated the optimal design of a film/foil capacitor having minimal losses and good heat transfer capability. However, a good capacitor design can be easily sabotaged by a poorly designed interconnection. Coil design is generally afforded a lot of attention, with thin insulated strands utilized to ensure the most optimal conductor usage subject to skin effect. The same issues also apply to the capacitor interconnections, which are pinch points for the resonating current. Traditional film capacitor lead diameters in the 18 to 20 gauge range are subject to skin effect restrictions at the higher frequencies under consideration for wireless charging. More suitable interconnections such as multi-stranded tinned-copper braids and copper or aluminum strap are necessary to avoid adding excess heat load to the capacitor. The connection to the extended capacitor foils is also a very critical aspect of the design. Using end-sprayed foil is the best approach to provide a robust current joint.

Thermal management

Wireless charging systems will generate heat due to losses in the solid state switching required to convert from grid frequency to the wireless power frequency along with the coil(s), capacitor(s), and interconnections. The relative contributions of these losses depend on the specific details of the system design, such as the compromise between coil current and capacitor voltage. The question of thermal management breaks down into two key aspects, namely extracting heat from the individual components and providing a thermal path to ambient that gives a manageable temperature rise for the total heat load.

Constructing a capacitor winding with minimal losses and good heat transfer characteristics can be readily undertaken as described in the previous sections. However, this strategy can backfire if the capacitor becomes a thermal conduit for additional heat, such as that generated by the coil or interconnections. In this situation, the hotspot temperature can readily be pushed

past the safe operating limit through no fault of the capacitor design and construction. Ideally, the heat extracted from each component should be transferred directly to the thermal ground rather than shared with neighboring components.

The thermal situation is particularly challenging for the grid side of the wireless charging system. The system will likely be buried in a garage floor or road bed with poorly defined coupling to a surrounding medium with highly variable thermal properties. In this condition, the entire system will float up to the temperature required to create a thermal gradient that can drive heat transfer to ambient and achieve equilibrium. As such, even with the lowest possible temperature rise in the capacitor, the safe limit can be readily exceeded by the system enclosure temperature offset from ambient. A high thermal resistance to ground can easily negate the perceived high temperature advantage of ceramic capacitors since the gap between 120°C for ceramic and 105°C for PP film becomes insignificant, even for a modest heat load. This problem can only be addressed by designing the thermal ground of the system so that the worst case thermal resistance and ambient temperature is defined.

CONCLUSIONS

The hybrid film/foil capacitor construction has been clearly shown to be the best choice for high power wireless charging over the range of 10 kHz to 150 kHz in terms of cost (50% of ceramic), performance (low-losses and high heat transfer), and reliability (self-healing). This approach combines the excellent thermal properties of foil in with the self-healing capability of a film dielectric using commercially available technology. Experimental testing of film/foil capacitor arrays has demonstrated that this design is very practical over the range of voltages and frequencies currently being pursued for wireless charging with suitable thermal boundary conditions. The film/foil approach is cost equivalent with double-metalized, and remains competitive with ceramic up to around 200 kHz where film dielectric loss becomes the limit. Furthermore, the film/foil construction minimizes electrode losses and enhances heat transfer from the capacitor hotspot for reduced system level cooling requirements. Ultimately, the capacitor performance must be considered at the system level with respect to stray field induction heating, optimal interconnections, and thermal management. With proper system level integration, film/foil capacitors represent a critical enabling technology for electric vehicle wireless charging. The SBE Power Ring Film Capacitor™ can take the film/foil approach to a next level of cost reduction using a large monolithic winding for each

stage of the capacitor array. This concept has already been adopted for the electric vehicle inverter market, where integration of the capacitor, interconnections and cooling provide reduced cost and size.

ACKNOWLEDGMENTS

The authors would like to recognize the contributions of Mr. Robert Backus at SBE, who was instrumental in setting up and running the capacitor testing program in support of this paper.

REFERENCES

1. Kurs, *et al.*, "Wireless Power Transfer via Strongly Coupled Magnetic Resonances," *Science*, **317**, 83, 2007.
2. Kurs André, "Power Transfer Through Strongly Coupled Resonances," Thesis, Master of Science in Physics, Massachusetts Institute of Technology, 77 Massachusetts Ave., Cambridge, MA, 02139-4307, September 2007.
3. Umenei, A.E., "Understanding Low Frequency Non-Radiative Power Transfer," Wireless Power Consortium contribution by Fulton Innovation LLC, 7575 Fulton Street East, Ada, MI, June 2011.
4. Sarjeant W.J., Zirnheld J., and MacDougall F.W., "Capacitors", *IEEE Transactions on Plasma Science*, Vol. 26, No. 5, October 1998.
5. Sarjeant W.J., Clelland I.W., and Price R.A., "Capacitive Components for Power Electronics, Proceedings of the IEEE, Vol. 89, No. 6, June 2001.
6. White W. and Galperin I., "Material Considerations for High Frequency, High Power Capacitors," *Transactions on Electrical Insulation*, Vol. EF-20, No.1, February 1985.
7. Bland M. J., Clare J. C., Wheeler P.W., "Multiphase Resonant Power Converter for High Energy Physics Applications," *Proceedings of EPAC 2006*, Edinburgh, Scotland.
8. Jung-gi Lee, Sun-kyoung Lim, Kwang-hee Namand Dong-ik Choi, "Design Method of an Optimal Induction Heater Capacitance for Maximum Power Dissipation and Minimum Power Loss Caused by ESR," *IEEE Transactions on Industry Applications*, Vol. 43, No. 4, July-August 2007.